

Coupled reaction channel analysis of $1n$ -pickup angular distribution in $^{32}\text{S} + ^{102,104}\text{Ru}$

Chandra Kumar^{1*} and S. Nath¹

¹Inter-University Accelerator Centre, Aruna Asaf Ali Marg, New Delhi 110067, India

Cross section of fusion (σ_{fus}) between two light ions can be described in terms of a potential model, in which the projectile and the target nuclei are considered to be inert. On the other hand, σ_{fus} of heavy ion reactions are known to be enhanced by orders of magnitude compared to the predictions of a simple potential model. Static and dynamic deformation of the collision partners have been invoked to explain sub-barrier enhancement of σ_{fus} . Coupled-channel models have been quite successful in taking into account the effects of coupling with inelastic channels. However, the role of nucleon transfer between the collision partners in influencing σ_{fus} is still not comprehensively understood. One approach is to measure the strong transfer channels and extract the form factors, which can then be incorporated in calculating σ_{fus} . Schindler *et al.* [1] measured one and two nucleon transfer cross sections for $^{32}\text{S} + ^{102,104}\text{Ru}$ and analyzed the data with a semiclassical coupled-channel model. Here we report coupled reaction channel (CRC) model analysis of $1n$ -pickup channel for these systems. More realistic description of transfer channels may lead to better estimates of form factors and, in turn, deeper understanding of their influence on σ_{fus} .

The theoretical study of angular distribution for $1n$ -pickup channel for the systems $^{32}\text{S} + ^{102,104}\text{Ru}$ at $E_{\text{lab}} = 110$ and 116 MeV was carried out using the code FRESCO [2]. The transition potential was calculated in the prior-representation including the full complex remnant terms. We generated this transition potential between the participating nuclei in the Woods-Saxon form, which was

taken from the global optical model potential (OMP) [3] for entrance and exit channels.

In the entrance channels, couplings of low-lying excited states and the ground states (g.s.) of the projectile and the target were included. Thus, the first excited states of the projectile and the targets, *v.z.*, $^{32}\text{S}_{2.230}$ (2^+), $^{102}\text{Ru}_{0.475}$ (2^+) and $^{104}\text{Ru}_{0.358}$ (2^+), were included in the entrance partitions. The nuclear and the quadrupole deformation for the projectile and the target had been taken from Ref. [4]. In order to construct the single particle bound wave function, the experimental binding energy for $1n$ -pickup channels was mimicked by changing the depth of the real part of the Woods-Saxon potential. The reduced binding radius and diffuseness for $\langle ^{33}\text{S}|^{32}\text{S} + 1n \rangle$ and $\langle ^{102,104}\text{Ru}|^{101,103}\text{Ru} + 1n \rangle$ were taken to be 1.30 fm and 0.70 fm nuclear cores, respectively. The one particle S.A. for projectile overlap was calculated using the code KSHELL code[5] considering ^4He as the inert core. The valence protons and neutrons were in the $1p_{1/2}$, $1p_{3/2}$, $1d_{3/2}$, $1d_{5/2}$ and $2s_{1/2}$ orbits. The monopole-based universal interaction was taken from Ref. [6]. Along with that, we also calculated the S.A. using *sd* model space with an effective phenomenological interaction [7].

S.A. for target overlap were taken from the data available in Ref. [8] and [9]. We also performed large-scale shell model (SM) calculations for $^{102,104}\text{Ru}$ using the jj45pna interaction and model space bearing the same name. ^{78}Ni was the core with valence protons in $1f_{7/2}$, $2p_{3/2}$, $1p_{1/2}$ and $1g_{9/2}$ orbits and neutrons in $1g_{7/2}$, $2d_{5/2}$, $2d_{3/2}$, $3s_{1/2}$ and $1h_{11/2}$ orbits. Due to computational limitations, we imposed some restrictions on the number of particles in different orbitals for protons as well as for neutrons. We allowed minimum

*Electronic address: dwngn10chandra@gmail.com

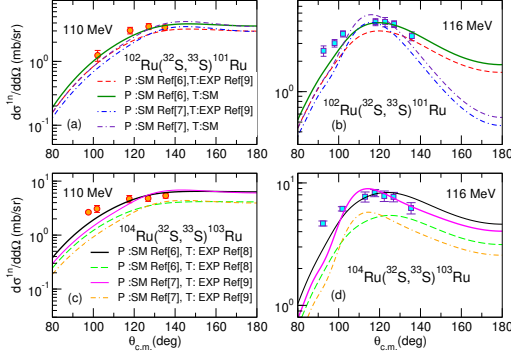


FIG. 1: Measured angular distributions for 1n-pickup channel, along with results of CRC calculations, for (a)–(b) $^{32}\text{S} + ^{102}\text{Ru}$ and (c)–(d) $^{32}\text{S} + ^{104}\text{Ru}$. P and T stand for projectile and target, respectively.

2 and maximum 10 protons in $1g_{9/2}$ orbital, whereas the $1f_{5/2}$ and $2p_{3/2}$ orbitals were fully occupied with protons. The minimum and the maximum number of neutrons allowed were, respectively, 3 and 6 in $2d_{5/2}$ orbital and zero in $1h_{11/2}$ orbital. All other members of the model space were unrestricted.

Results of CRC calculations for $^{102}\text{Ru}(^{32}\text{S}, ^{33}\text{S})^{101}\text{Ru}$ are shown in Fig. 1(a) and (b). The g.s. to g.s. transition was found to play an important role, however, the cross sections were still underpredicted. The data were well reproduced when the couplings between both the g.s. and the inelastic state $^{33}\text{S}_{0.840}(1/2^+)$ were included in the final partition. We used S.A. computed with *psd* and *jj45pna* model spaces for projectile-like and target-like nuclei, respectively.

For $^{104}\text{Ru}(^{32}\text{S}, ^{33}\text{S})^{104}\text{Ru}$, results of CRC calculations are shown in Fig 1(c) and (d). Similar to the case of $^{28}\text{Si} + ^{102}\text{Ru}$, major contribution to the cross sections came from g.s. to g.s. transition. We further included the inelastic states of both the projectile-like and the target-like nuclei. In the final partition, $^{33}\text{S}_{g.s.}(1/2^+)$, $^{33}\text{S}_{0.840}(1/2^+)$, $^{33}\text{S}_{1.967}(5/2^+)$ and $^{103}\text{Ru}_{g.s.}(5/2^+)$, $^{103}\text{Ru}_{0.136}(5/2^+)$, $^{103}\text{Ru}_{0.174}(1/2^+)$, $^{103}\text{Ru}_{0.213}(7/2^+)$ states were included. It appears from CRC results that more inelastic states contribute to the

cross sections in case of the system having a collision partner with larger deformation, *i.e.*, ^{104}Ru ($\beta_2 = 0.274$) as compared to ^{102}Ru ($\beta_2 = 0.1707$).

From Fig. 1(b), it is clearly visible that S.A. obtained from Refs. [6, 7] and Ref. [8] for projectile-like and target-like nuclei, respectively, reproduced the angular distribution for $^{104}\text{Ru}(^{32}\text{S}, ^{33}\text{S})^{104}\text{Ru}$ well. It is observed that the CRC calculations at $E_{\text{lab}} = 116$ MeV for both systems that the angular distributions have different shapes for two different interactions used in the SM for ^{32}S . One shows a broad angular distribution [6] while the other shows a narrower and somewhat bell-shaped angular distribution [7]. This signifies that angular distribution for 1n-pickup channel depends strongly on the structure of ^{32}S and results of SM calculations.

In conclusion, the CRC results depend on many factors such as S.A., binding potential and OMP. The larger deformation of the target appeared to cause coupling with many inelastic states. A systematic study of transfer channels, within the CRC framework, for a large number of systems may be useful in reducing the uncertainties in the results. Clearer understanding of few nucleon transfer would also lead to better explanation of how particle transfer channels affect sub-barrier fusion dynamics.

C.K. acknowledges financial support from the Council of Scientific and Industrial Research (CSIR), New Delhi via grant no. CSIR/09/760(0038)/2019-EMR-I. The High Power Computing Facility of IUAC was utilised for performing all calculations.

References

- [1] F. J. Schindler *et. al.* Nucl. Phys. A **603**, 77 (1996).
- [2] Ian J. Thompson, Comput. Phys. Rep. **7**, 167 (1988).
- [3] A. V. Karpov *et. al.*, Nucl. Instrum. Methods A **859**, 112 (2017).
- [4] S. Raman *et. al.*, At. Data Nucl. Data Tables **78**, 1 (2001).
- [5] N. Shimizu *et. al.*, Comput. Phys. Commun. **244**, 372 (2019).
- [6] C. Yuan *et. al.*, Phys. Rev. C **85**, 064324 (2012).
- [7] B. A. Brown and B. H. Wildenthal, Annu. Rev. Nucl. Part. Sci. **38**, 29 (1988).
- [8] H. T. Fortune *et. al.*, Phys. Rev. C **3**, 337 (1971).
- [9] J. L. M. Duarte, *et. al.*, Phys. Rev. C **50**, 666 (1994).